

Synthesis of Fluorescent Hollow Silica Nanoparticles and Application in Detecting Hypochlorite

Gang Wang,¹ Yue-Hong Zhu,¹ Guang-Gai Zhou,¹ Wei-Liang Liu,^{*1} Xian Zhang,¹ Xiao-Xia Cai,¹ Qin-Ze Liu,¹ and Xin-Qiang Wang²

¹*School of Materials Science and Engineering, Qilu University of Technology, Jinan 250353, P. R. China*

²*State Key Laboratory of Crystal Materials, Shandong University, Jinan 250100, P. R. China*

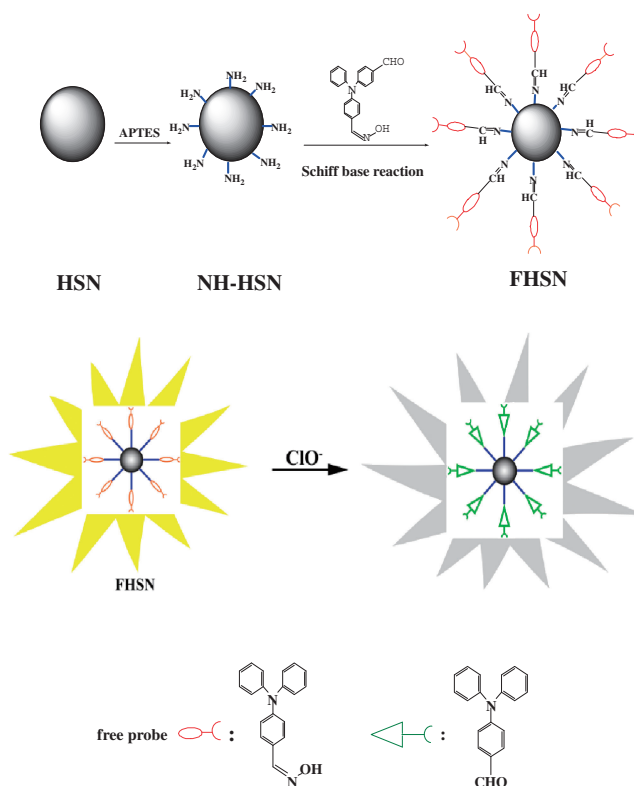
(E-mail: wlliu@sdu.edu.cn, liuw1@qlu.edu.cn)

In this paper, fluorescent hollow silica nanoparticles (FHSNs) have been used for the detection of hypochlorite by monitoring fluorescence intensity changes. The fluorescent and sensing properties of the FHSNs were dramatically improved compared to those of the corresponding free probes. With unique hollow structure and strong fluorescence, the FHSNs have potential applications in the fields of biology and medicine.

Reactive oxygen species (ROS) play significant roles in physiological processes.¹ Hypochlorite anion (ClO^-), as one of the more important ROS, is involved in our bodily functions and other aspects of our daily lives. Biologically, ClO^- is well-known for its unique antibacterial properties in the immune system and can also mediate the chemical modification of various biomolecules.² In our daily life, ClO^- and hypochlorous acid are widely used as disinfectants or bleaching agents for water. However, it has been proved that over-production of and excessive intake of ClO^- can be dangerous to humans. On one hand, over-production of ClO^- in living organisms can cause many diseases such as carcinogenesis and inflammation. On the other hand, disinfected water with residual chlorine may cause stomach discomfort and irritation of the eye or nose.³ To this effect, a number of sensitive and selective analytical fluorescent chemosensors have been synthesized for conducting such research, but some of them fail to fulfill the appropriate criteria for imaging endogenous ClO^- .^{4,5}

In recent years, owing to its controllable uniform size, good biocompatibility, and less toxicity, fluorescent silica nanoparticles (FSNs) encapsulated by organic fluorophores have attracted considerable attention from the fields of medical technology and biological sciences.⁶ Owing to fast energy transfer and efficient nonradiative rate, the fluorescence of the FSNs tends to be quenched faster than the corresponding free dyes.⁷ We therefore wanted to introduce organic fluorescent probes on the surface of silica nanoparticles. Furthermore, the unique hollow structures enable the silica nanoparticles to encapsulate functional compounds and medicinal compounds, which may make them potential “detection-cure” materials for ClO^- -caused disease. In this study, we have introduced a fluorescent probe on the surface of hollow silica nanoparticles (HSNs) to assemble fluorescent hollow silica nanoparticles (FHSNs) for the detection of ClO^- . The procedure for preparing FHSNs and their application in detecting ClO^- is described in Scheme 1. The synthetic routes to FHSNs and the corresponding free probes are shown in Supporting Information.

The morphology and structure of HSNs and FHSNs are presented in Figure 1. Both the HSNs and FHSNs exhibit a uniform, discrete, and hollow spherical shape with an average diameter of 80 nm. Additionally, the uncoated HSNs are smooth and spherical, shown in Figure 1a; in contrast, functionalized



Scheme 1. The procedure for preparing FHSNs and application in detecting hypochlorite.

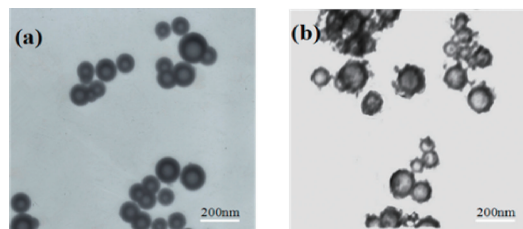


Figure 1. TEM images of HSNs (a) and FHSNs (b).

with the free probe, FHSNs show a noticeable difference in their surface texture, which presented uneven multilayer coatings, as exhibited in Figure 1b. The functionalization on the structure of HSNs was investigated by EDS and FT-IR analysis (Figure S1).

In order to simulate the physiological condition, the fluorescence properties were investigated upon adding different volumes of ClO^- to FHSNs in Tris-HCl buffer solution of pH 7.2. The experimental results are displayed in Figure 2. Compared to the original compound, no obvious red-shifts or

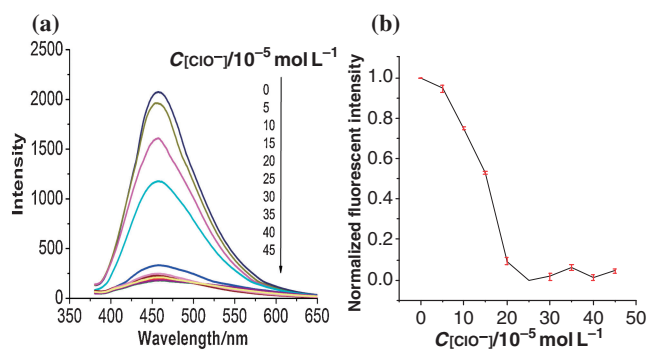


Figure 2. (a) Fluorescence emission spectra of FHSNs (0.2 g L^{-1}) in the presence of different concentrations of hypochlorite anion ($0\text{--}4.5 \times 10^{-4} \text{ mol L}^{-1}$) in 0.01 mol L^{-1} Tris-HCl buffer solution, pH 7.2. (b) The normalized fluorescent intensity at 457 nm evolution with ClO^- concentrations.

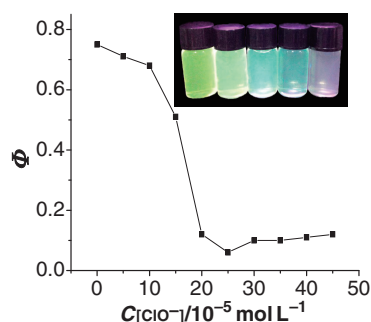


Figure 3. Quantum yields (Φ) of FHSNs (0.2 g L^{-1}) in the presence of different concentrations of hypochlorite anion ($0\text{--}4.5 \times 10^{-4} \text{ mol L}^{-1}$) in 0.01 mol L^{-1} Tris-HCl buffer solution, pH 7.2. Inset at (a): photographs of solutions of FHSNs in the presence of different concentrations of hypochlorite from low (left) to high (right), taken under UV illumination (365 nm).

blue-shifts were observed with increasing ClO^- concentrations (Figure 2a). Fluorescent intensity decreased dramatically with the addition of ClO^- up to a concentration of $2.5 \times 10^{-4} \text{ mol L}^{-1}$, then leveled off (Figure 2b). To check the reproducibility of the FHSNs, the above experiments were repeated thrice. The error bars were small and the reproducibility was relatively good. The limit of detection (LOD) was estimated to be $1.77 \times 10^{-8} \text{ mol L}^{-1}$. (see detailed calculation of LOD in Supporting Information).

To quantitatively determine the fluorescent intensity of FHSNs as a function of ClO^- concentration, quantum yields (Φ , see Supporting Information) in the presence of different concentrations of ClO^- were calculated (Figure 3). As demonstrated in Figure 3, quantum yields decreased with increasing ClO^- concentration, then leveled off when the concentration was over $2.5 \times 10^{-4} \text{ mol L}^{-1}$, in accordance with the progressively weaker emissions, as shown in the photos of the solutions taken in dark upon excitation by a UV lamp at the wavelength of 365 nm.

The mechanism for detecting the ClO^- of FHSNs was also investigated, which was the $-\text{CH}=\text{N}-\text{OH}$ reacted with ClO^- and formed the new $-\text{CHO}$ group in the detection process.

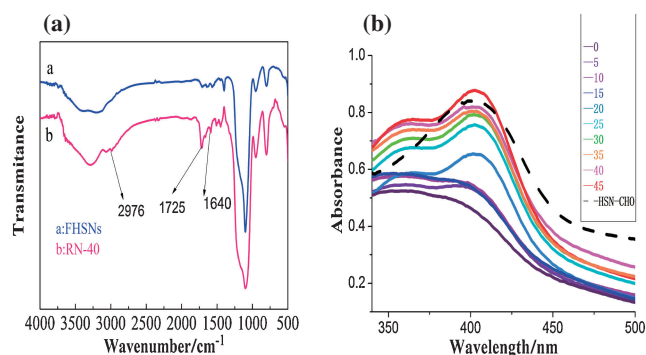


Figure 4. (a) FT-IR spectra of FHSNs and RN-40. (b) UV-vis spectra of FHSNs in the presence of different concentrations of hypochlorite anion ($0\text{--}4.5 \times 10^{-4} \text{ mol L}^{-1}$) and HSN-CHO.

The FHSNs, after reaction with ClO^- (concentration: $40 \times 10^{-5} \text{ mol L}^{-1}$), were collected by centrifugation, washing, and vacuum drying (denoted as RN-40). RN-40 was studied by FT-IR analysis (Figure 4a). The peak shape and position of RN-40 remained almost the same as that of FHSNs. The absorption peaks at about 1640 and $2900\text{--}3000 \text{ cm}^{-1}$ confirmed that the $-\text{C}=\text{N}$ bond and $-\text{CH}_2$ group also existed in the RN-40. However, in the RN-40 spectrum, a new absorption peak appeared at 1725 cm^{-1} , which belonged to the $-\text{C}=\text{O}$ stretching vibration in the $-\text{CHO}$ group. UV-vis spectral analysis of FHSNs was also carried out upon adding different volumes of ClO^- to FHSN in Tris-HCl buffer solution (Figure 4b). The original FHSNs have a wide absorption at about 351 nm . When only a small amount of ClO^- ($5\text{--}10 \times 10^{-5} \text{ mol L}^{-1}$) was added, the shape and position of the absorption peaks remained almost the same. However, when the concentration reached $15 \times 10^{-5} \text{ mol L}^{-1}$, a new absorption peak appeared at 403 nm ; further increasing the ClO^- concentration to $20 \times 10^{-5} \text{ mol L}^{-1}$, the new peak became prominent and intensity of the new peak increased with further increase in ClO^- concentration ($25\text{--}45 \times 10^{-5} \text{ mol L}^{-1}$). This may suggest that one new species was formed during the titration process.

To further confirm the structure of the new species, imitating the procedure of preparing FHSNs, we introduced 4,4'-diformyltriphenylamine on the surface of HSNs, giving aldehyde-containing HSNs (denoted as HSN-CHO). The UV-vis spectral analysis of HSNs-CHO was performed under the same conditions as that of FHSNs (Figure 4b). Interestingly, the new peak position was identical to that of the HSN-CHO. Both the FT-IR and UV-vis spectra demonstrated the $-\text{CH}=\text{N}-\text{OH} \rightarrow -\text{CHO}$ mechanism. Furthermore, fluorescent effect experiment of HSN-CHO showed that the emission of HSN-CHO was hardly detectable.

The fluorescence properties of the corresponding free probe were also investigated (Figure S3). The photophysical data of FHSNs and the corresponding free probe are summarized in Table 1. Compared to the free probe, the UV absorbance was red-shifted by 67 nm . Meanwhile, it can be found that Φ of FHSNs was 3 times larger than that of the free probe. The LOD of the FHSNs ($1.77 \times 10^{-8} \text{ mol L}^{-1}$) is much lower than that of the free probe ($2.3 \times 10^{-6} \text{ mol L}^{-1}$) (see Supporting Information). All of these data implied that FHSNs were more suitable for medical and biological use.

Table 1. UV absorption and OP fluorescent spectrum related photophysical data of different systems

| | Φ | $\lambda_{\text{max}}^{\text{UV}}/\lambda_{\text{max}}^{\text{OP}}$ | LOD/mol L ⁻¹ |
|--------------------------|--------|---|-------------------------|
| FHSN | 0.75 | 403/457 | 1.77×10^{-8} |
| Corresponding free probe | 0.26 | 336/455 | 2.3×10^{-6} |

All the differences suggested that the fluorescence properties and sensitivity of the free probe can be improved effectively by being introduced on the surface of HSNs. The main mechanism of the improved property of the FHSNs can be attributed to free probe being fixed on the surface of the HSNs, which weakens the molecular vibration and rotation of the probe when the probe molecules were excited. The non-radioactive transition is weakened, which leads to the increase of the quantum yield. As for the bathochromic shift observed in the absorption spectra of FHSNs, we deduced the possible reason may be that when connecting the free probe on the surface of the nanoparticles by Schiff-base reaction, a large number of -C=N double bonds are formed in the FHSNs (Scheme 1). According to the molecular orbital theory, with the increase in the number of -C=N bonds, the bonding orbital energy was raised, whereas the antibonding orbital energy gradually decreased, and the energy needed for electron transition (ΔE) decreased, so the absorption peak suffered a bathochromic shift in the FHSN spectra. The difference of LOD may be attributed to the fact that a single probe can merely react with only one ClO^- and the possibility for their contact is relatively low in solution.

However, owing to a large number of probes being attached on its surface, a single FHSN, as a whole, has more chance of coming into contact with a single ClO^- , making the probes much easier to be destroyed by ClO^- in comparison to that of a single probe in solution, which leads to the decrease of the LOD.

In summary, by synthesizing a new fluorescent probe and introducing it on the surface of HSNs, we have successfully prepared FHSNs for the detection of ClO^- . The fluorescent and sensing properties of the FHSNs are superior to those of the corresponding free probe. In the future, by encapsulating anti- ClO^- drugs into the unique hollow structure with strong fluorescence effect, the FHSNs may exhibit great potential for application in biological and medical fields.

Supporting Information is available electronically on J-STAGE.

References

- 1 B. C. Dickinson, C. J. Chang, *Nat. Chem. Biol.* **2011**, *7*, 504.
- 2 H. Wiseman, B. Halliwell, *Biochem. J.* **1996**, *313*, 17.
- 3 J. Zhang, X. Yang, *Analyst* **2013**, *138*, 434.
- 4 J. Shi, Q. Li, X. Zhang, M. Peng, J. Qin, Z. Li, *Sens. Actuators, B* **2010**, *145*, 583.
- 5 B. Zhu, Y. Xu, W. Liu, C. Shao, H. Wu, H. Jiang, B. Du, X. Zhang, *Sens. Actuators, B* **2014**, *191*, 473.
- 6 G. Chen, F. Song, X. Wang, S. Sun, J. Fan, X. Peng, *Dyes Pigm.* **2012**, *93*, 1532.
- 7 S.-W. Ha, C. E. Camalier, G. R. Beck, Jr., J.-K. Lee, *Chem. Commun.* **2009**, 2881.